

Cellulose acetate/cellulose nanofiber membranes for whey and fruit juice microfiltration

Liliane Cristina Battirola  · Patrícia Fernanda Andrade · Gabriela Vollet Marson · Miriam Dupas Hubinger · Maria do Carmo Gonçalves

Received: 5 June 2017 / Accepted: 22 September 2017 / Published online: 13 October 2017
© Springer Science+Business Media B.V. 2017

Abstract Asymmetric membranes based on cellulose acetate (CA) and cellulose nanofibers (CNF) were prepared by non-solvent induced phase separation. The effect of CNF addition on the morphology, water flux and filtration performance of the CA membranes was investigated. Field emission scanning electron micrographs showed the formation of large macrovoids at low CNF content, while the increase of the CNF content resulted in a sponge-like morphology due to changes in the demixing process rate during membrane formation. Porosity and pure water flux increased with the increment of CNF content. In addition to this, molecular weight cut-off was 200 kg mol^{-1} for nearly all composite membranes studied. CA/CNF5 composite membranes were also tested to clarify strawberry and raspberry juices as well as whey. Clarification of fruit juices and whey was shown by the decrease of turbidity and solid content. Moreover, the maintenance of antioxidant capacity, as well as overall color for strawberry and raspberry juices, could be seen

leading to the conclusion that this composite membrane can be useful in juice production.

Keywords Cellulose acetate · Cellulose nanofibers · Membrane separation · Microfiltration · Phase inversion · Juice clarification

Introduction

Cellulose esters have great potential as membranes for separation processes. As of the last four two decades until now, cellulose acetate (CA) has been applied in different aqueous separation processes such as reverse osmosis (Kunst and Sourirajan 1974; Perera et al. 2014) and ultrafiltration (Kutowy and Sourirajan 1975; Han et al. 2013), mainly due to its interesting characteristics, such as the hydrophilicity, hardness and relatively low cost. In separation processes, CA membranes have shown satisfactory results such as for trace organic contaminant removal (He et al. 2015), and separation of biomolecules or complex heavy metals (Soylak et al. 2002, 2010; Chen et al. 2004; Divrikli et al. 2007). However, in order to increase the selectivity or the mechanical properties of CA membranes, blends and composite membranes based on CA have been prepared (Tian et al. 2011; Abedini et al. 2011; Andrade et al. 2015).

In this context, nanocelluloses can be a good candidate as fillers for CA composite membrane

L. C. Battirola · P. F. Andrade · M. C. Gonçalves (✉)
Institute of Chemistry, University of Campinas
(UNICAMP), P. O. Box 6154, Campinas, SP 13083-970,
Brazil
e-mail: maria@iqm.unicamp.br

G. V. Marson · M. D. Hubinger
Department of Food Engineering, School of Food
Engineering, University of Campinas (UNICAMP),
Campinas, SP 13083-862, Brazil

preparation. Cellulose nanofibers (CNF) are long, flexible and entangled and are made up of individualized cellulose nanofibrils, presenting 10–100 nm lateral dimensions and length generally in the micrometer scale. This cellulosic material consists of alternating crystalline (cellulose) and amorphous domains (lignin and hemicellulose), and has been indicated for applications in many areas such as paper making (Nogi et al. 2009), coating (Aulin et al. 2010), packaging (Spence et al. 2010) and gas barriers (Fukuzumi et al. 2009). The numerous possible applications are justified by the renewable character, high aspect ratio, low thermal expansion, low cost and relatively easy production (Abdul Khalil et al. 2014). CNF can be extracted from natural fibers by mechanical methods, such as grinding, high-pressure homogenization, microfluidization and sonication, by chemical methods, such as fermentation (Kalia et al. 2014), or the combination of some of them. As a reinforcing filler in the polymers, CNF has been mixed with different polymer matrices, such as poly(lactic acid) (Iwatake et al. 2008), polyurethane (Özgür Seydibeyoğlu and Oksman 2008), poly(ethylene oxide) (Fortunato et al. 2012) and starch (Takagi and Asano 2008). Although the use of cellulose fibers in different polymers has already been proven to be an important strategy for obtaining nanocomposites with improved mechanical performance, these nanoreinforcements also offer possibilities such as additives for membrane development. Kong et al. (2014) have shown that the addition of oxidized CNF to cellulose tri-acetate promoted an increase in membrane hydrophilicity, also resulting in an increase in water flux. Even though the results obtained by these same authors were interesting, no proposals were made in terms of their application.

Membranes can be produced by phase inversion methods, which can be described as a demixing process whereby the initially homogeneous polymer solution is submitted to a liquid–solid phase transition in a controlled manner. This transformation can be made by the immersion of a polymer solution in a non-solvent bath (non-solvent induced phase separation—NIPS). The NIPS method is one of the most popular membrane formation methods because it allows the preparation of asymmetric membranes with different morphologies. Asymmetric CA membranes produced by using NIPS show macro-voids and sponge-like morphologies, depending on the polymer solution

composition, the preparation conditions and the presence of additives (Reuvers and Smolders 1987; Guillen et al. 2011; Lalia et al. 2013).

Microfiltration, ultrafiltration and reverse osmosis have been widely applied to the dairy, food and beverage industry, mainly to improve shelf-life and concentrate liquids such as juices, wine, beer, oils and syrups and, in addition to this, they are also used to purify and fractionate protein solutions (Ghosh 2008; Belleville and Vaillant 2015). Membrane separation processes have advantages such as a reduction in energy consumption, lower capital investments and they are also usually performed at low temperatures involving little or no deterioration of the compounds (Belleville and Vaillant 2015). Microfiltration has been used as a pre-treatment to remove fine suspended particles from biological products (Qiu et al. 2015; Arend et al. 2017). This can prevent fouling in further membrane separation stages (Campos et al. 2016) and also result in clarified products which can be used as ingredients in beverages, candies and other food preparation (Qiu et al. 2015).

In this work, the effect of CNF incorporation on the CA asymmetric membrane performance was investigated. Focus has been put on the characterization of membrane morphology and water permeation flux as well as membrane filtration performance, which was assessed in fruit juices and whey regarding their total and soluble solids, color, turbidity, antioxidant activity and total phenolics.

Experimental section

Materials and techniques

Cellulose nanofiber (CNF) from Eucalyptus kraft pulp was kindly supplied by Suzano Papel e Celulose S.A., Limeira, Brazil. Cellulose acetate (CA) (Eastman Chemicals Co.), free of additives, with a 50 kg mol^{-1} number-average molecular weight and 38.7 wt% acetyl group was dried under vacuum at $60 \text{ }^\circ\text{C}$ overnight prior to use. Acetone (99%, Lab synth) was used as received. Absolute alcohol, polyethylene glycol (20, 35, 100 and 200 kg mol^{-1} molecular weights), gallic acid, TPTZ (2,4,6-tris(2-pyridyl)-s-triazine), 97% pure TROLOX (6-hydroxy-2,5,7,8-tetramethylchroman-2-carboxylic acid), Folin's reagent, sodium carbonate, sodium acetate and ferric

chloride presented analytical grade. The deionized water used in all experiments was supplied by a Millipore system. Strawberry (lote #06215/11, DeMarchi Ind. e Com. de Frutas Ltda.), red raspberry (lote #95053/01, DeMarchi Ind. e Com. de Frutas Ltda.) pulps, pasteurized milk and full-fat yogurt were purchased from a local supermarket.

Preparation of the cellulose acetate membrane

All membranes were prepared using the non-solvent induced phase separation process. CA (5.0 g) was solubilized in acetone (38.0 mL) at 50 °C. After homogenization of the polymer solution, water (10.5 mL) was added and left to stir for 24 h. Following that, the polymer solution was spread over a 20 cm × 30 cm glass plate surface, containing two 200 mm thick nickel–chromium wires stretched laterally, used to control membrane thickness. The film was allowed to evaporate for 20 s before being dipped into deionized water (coagulation bath) maintained at room temperature (approximately 25 °C), to allow membrane formation. After polymer precipitation, the membrane was dried at room temperature.

Preparation of acetate cellulose membranes with cellulose nanofiber

Membranes containing CNF were prepared by using the same procedure as the pure CA membrane. Cellulose acetate (5.0 g) was dissolved in acetone (38.0 mL) at 50 °C under constant stirring. Different amounts of nanofiber were added to the CA solution using 3 wt% CNF suspension. The weight content of the polymer, acetone and water in the casting solution was kept constant (11:66:23) for all solutions. The CNF contents, in relation to CA, were 1.2, 2.5, 5.0 and 10.0 wt%. The composite membranes were labeled as CA/CNFX, where the X denotes the amount of CNF.

Preparation of fruit juices and whey

Fruit juices were prepared by mixing ultra-pure water and pulp in a blender (Corning laboratory blender) in the 1:2 weight proportion, respectively. Fruit juices were centrifuged in an Allegra 25-R, Beckman Coulter centrifuge, at 10,000 rpm for 30 min at 4 °C, in order to remove suspended solids. Whey was obtained from homemade dry curd, which was prepared using

pasteurized milk and natural yogurt with no additives, apart from the microbial culture. Milk was fermented by the culture present in the yogurt for 1 day at 15 ± 1 °C, filtered in a sterilized cotton bag and then centrifuged at 10,000 rpm for 30 min at 4 °C. All samples were prepared on the day of membrane separation. The feed, permeate and retentate were stored in a freezer (−18 °C) until analysis.

Characterization of cellulose nanofiber and membranes

CNF morphology was examined in a transmission electron microscope (TEM) (Carl Zeiss Libra 120) equipped with an in-column OMEGA filter, at an acceleration voltage of 120 kV. Drops of diluted aqueous CNF suspensions were deposited on carbon coated parlodion films supported on copper grids and allowed to dry. CNF dimensions were measured using the ImageJ software. The morphology of the cryogenically fractured membranes was examined in a field emission scanning electron microscope (SEM) (Fei Quanta FEG-250) operating at a 5 kV accelerating voltage. The CNF morphologies were also examined by dropping a CNF aqueous suspension on a mica surface mounted in the sample holder. All samples were carbon and platinum sputter coated in a Bal-Tec MD 020 (Balzers).

The thermal stability of the samples was determined by thermogravimetric analysis (TGA) using a TGA 2950 TA instrument thermo-balance, under an argon atmosphere (100 mL min^{−1} flow rate), and heated at 25–900 °C (at 10 °C min^{−1}).

Water contact angle measurements were carried out using drop shape analysis equipment (Krüss Easy drop DSA 20). A sessile drop formed by deionized water was deposited on the top membrane surface and the contact angle value was recorded. Measurements were performed at room temperature (~24 °C) and repeated using 10 different fresh top surfaces. Membrane porosity was measured using the dry–wet weight method, proposed by Chen et al. (2004). Initially, 6 square sections with 1 cm × 1 cm dimensions of approximately the same weight were immersed in a deionized water thermostatic bath at 25 °C for 6 h, and weighed in an AD-6 microbalance (Perkin-Elmer). Then, they were weighed again after vacuum drying for 24 h at 60 °C. The porosity was calculated according to the following equation:

$$\text{Porosity (\%)} = \left[\frac{\frac{W_w - W_d}{\rho_w}}{\frac{W_w - W_d}{\rho_w} + \frac{W_d}{\rho_p}} \right] \times 100 \quad (1)$$

where W_w is the wet membrane weight (g), W_d is the dry membrane weight (g), ρ_w is density of pure water at 25 °C (0.997 g cm⁻³) and ρ_p is the density of the polymer at 25 °C (1.33 g cm⁻³).

A dead-end filtration cell (300 mL) was used to measure pure water flux through each membrane, using deionized water at room temperature. To do so, an especially custom made apparatus designed for membrane characterization at a laboratory scale was used (Andrade et al. 2015). Membranes (1662 mm²) were sealed with O-rings and fixed between two steel parts. A magnetic stirrer, located under the membrane cell, allowed a speed of 300 rpm. The membranes were conditioned for 15 min at 9.0 ± 0.5 bar, prior to the tests. Continuous measurements of the membrane permeate flux were carried out by collecting the permeated water and measuring its volume at regular intervals. Pure water flux was calculated as follow:

$$J = \frac{V}{A\Delta t} \quad (2)$$

where J is the pure water flux (L m⁻² h⁻¹), V is the water permeated volume (L), A is the membrane surface area (m²), and Δt is the permeation period of time (h). The experiments were carried out at 25 ± 1 °C and 10 ± 1 bar pressure provided by compressed nitrogen gas, except for CA/CNF10.0. In this case, pure water flux experiments were carried out at 3.0 bar pressure. Measurements were carried out at least seven times.

Membrane molecular weight cut-off (MWCO) was determined in the same apparatus used to determine pure water flux, by feeding the apparatus with dilute aqueous polyethylene glycol (PEG) solutions of different number-average molecular weights: 20, 35, 100 and 200 kg mol⁻¹. In this work, MWCO was taken as the molecular weight of polyethylene glycol where the membrane has rejection at around 80%. The percentage solute rejection, %SR, was found using the following equation:

$$\%SR = 1 - \frac{C_p}{C_f} \times 100 \quad (3)$$

where C_p and C_f are the concentrations of the solute in permeate and feed solutions, respectively. Total organic carbon content was determined from all PEG solutions in the feed and permeate samples using a TOC-V CPN Shimadzu equipment.

Membrane separation of juices and whey

Fruit juices and whey were filtered in the same apparatus used to measure the water flux of the membranes. Moreover, whey samples were also submitted to a test in a 2 L capacity tangential filtration system (Invict, Mentest), with an effective permeation area of 7700 mm². Feed stream was pumped into a tank with controlled temperature (model TE-184, Tecnal). Experiments were conducted at 7.5 ± 0.5 bar and 25 ± 1 °C. Initial feed volume was 300 mL and the concentration process was carried out until the concentration factor reached the value of six. The concentration factor was calculated by Eq. 4. Permeate flux was calculated by Eq. 2.

$$CF = \frac{V_f}{V_f - V_p} \quad (4)$$

where V_f and V_p are the volume of feed solution and permeate solution, respectively.

Juices and whey characterization

Turbidity, color, soluble solids, total solids and pH were measured for feed, permeate and retentate of all the samples. Antioxidant capacity and total phenolics were measured for the juices. Briefly, turbidity was measured using a UV-Vis spectrophotometer (model 2800, Unico) as described by Silva et al. (2010) and expressed as a 660 nm absorbance (Gökmen et al. 2001). Color was measured in an UV-Vis spectrophotometer in reflectance mode (D65 illuminant, model UltraScan, Hunterlab). Results were expressed as the parameters of the CIELab scale where L^* represents the luminosity ($L = 0$ corresponds to the darkest black and $L = 100$ to the brightest white), a^* represents the green (-)/red (+) colors and b^* the blue (-)/yellow (+) colors. Color difference values were calculated to study color changes. Total color difference (ΔE^*) was defined as:

$$\Delta E = [(L_p^* - L_r^*)^2 + (a_p^* - a_r^*)^2 + (b_p^* - b_r^*)^2]^{0.5} \quad (5)$$

where L_p^* , a_p^* and b_p^* are the corresponding values for the permeate solutions and L_r^* , a_r^* and b_r^* are the corresponding values for the retentate solutions. Analyses of color changes between permeate and feed solutions were also carried out. In this case, L_r^* , a_r^* and b_r^* were replaced by L_f^* , a_f^* and b_f^* .

Total solids, soluble solids and pH were determined as described by the Association of Official Analytical Chemists (AOAC 2006). Briefly, total solids were determined by weight after drying the samples in an incubator for 12 h at 105 °C (model C-HT 515 Orion, Fanem). Soluble solids were measured at 25 °C with a refractometer (model N-1 alpha, ATAGO) and expressed as brix degrees (°Bx), pH at 25 °C was measured in an pHmeter (Kasvi).

Antioxidant capacity was determined by the Ferric Reducing Ability of Plasma (FRAP assay), as described by Benzie and Strain (1996) and the changes proposed by Rufino et al. (2006). FRAP reagent was prepared at the time of the assay by mixing the acetate buffer solution (0.3 M, pH 3.6), TPTZ solution (10 mM diluted in HCl 40 mM) and ferric chloride (20 mM diluted in distilled water) in a 10:1:1 proportion, respectively. Trolox was used as standard. In a dark environment, 2.25 mL FRAP reagent, 225 μ L water and 75 μ L sample (or distilled water for the blank) were mixed and incubated at 37 °C for 30 min

in a water bath (model TE-184, Tecnal) and then read at 595 nm in the spectrophotometer (model 2800, Unico). Results were expressed as TROLOX equivalents, in mg mL^{-1} . Total phenolics were determined by the Singleton and Rossi method (1965) as described by Waterhouse (2003). Briefly, a 40 μ L sample (or distilled water for the blank) was mixed with 3.16 mL water and 200 μ L Folin reagent for 5 min. Then 600 μ L sodium carbonate solution (250 g L^{-1}) was added and the mixture was left to react for 2 h and then read at 765 nm in a spectrophotometer (model 2800, Unico). Gallic acid was used as standard and results were expressed as gallic acid equivalents (GAE), in mg mL^{-1} .

All analyses were performed in triplicate. One-way analysis of variance (ANOVA) followed by the unpaired Tukey's *t* test was used, and $p < 0.05$ was considered statistically significant.

Results and discussion

The CNF morphology was observed by TEM and SEM. Representative images are shown in Fig. 1a, b. The nanofiber diameter was measured as being in the 20–150 nm range, with a 50 ± 20 nm average diameter.

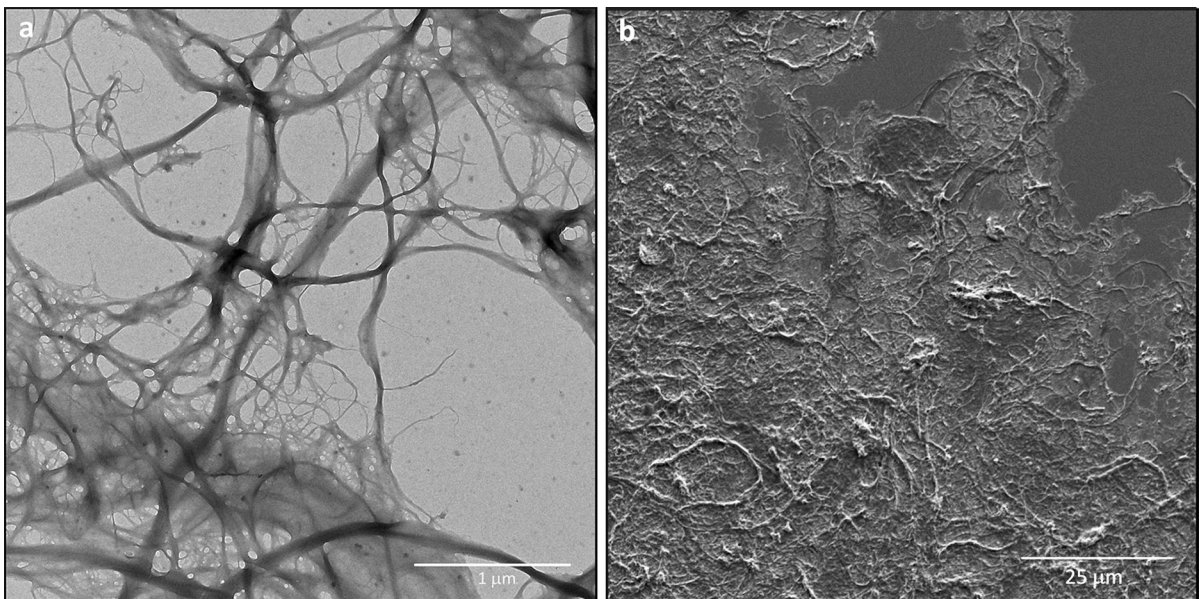


Fig. 1 CNF **a** TEM and **b** SEM micrographs

Table 1 Initial thermal degradation temperature (T_{onset}) for pure CA membrane, CNF and CA/CNF membranes

Sample	T_{onset} (°C)
CA	340
CA/CNF1.2	320
CA/CNF2.5	319
CA/CNF5.0	310
CA/CNF10.0	307
CNF	273

Table 1 shows the initial thermal degradation temperature for CNF, CA matrix and CA/CNF composite membranes. Natural fibers are made up of cellulose (crystalline component), hemicelluloses and lignin, which are non-crystalline. In natural fibers, the thermal degradation of the non-crystalline components starts at lower temperatures when compared to the crystalline cellulose. CNF presented one thermal degradation event at 273 °C, which is currently related to cellulose degradation processes such as depolymerization, dehydration, and decomposition of the glycosyl units followed by the formation of a charred residue (Roman and Winter 2004). On the other hand, the pure CA membrane presented a main weight loss event at 340 °C, which is related to the thermal degradation of the cellulose acetate main chain. Huang and Li (1998) showed that the presence of acetyl groups increases the thermal stability of cellulosic materials compared to natural cellulose. The presence of CNF non-crystalline components in CA composite membranes was responsible for the decrease of the onset degradation temperature, as a consequence of hemicellulose presence as reported by Yang et al. (2007).

In order to investigate the influence of introducing CNF on CA membrane morphology, micrographs of the CA and CA/CNF membrane cross-sections were obtained by SEM (Fig. 2). Significant membrane morphological changes could be observed. According to the image in Fig. 2a, the pure CA membrane presented typical macrovoid and sponge-like structures along the bulk region. The addition of a low CNF content (from 1.2 to 2.5 wt%) also resulted in the formation of large macrovoids (Fig. 2b, c). However, a further increase of the CNF content, from 5.0 to 10.0 wt%, promoted the suppression of the macrovoid formation, leading to preferentially a sponge-like structure (Fig. 2d, e). Sabeti Dehkordi et al. (2015) reported similar results by adding organically

modified clay into the CA membrane. The presence of the hydrophilic filler in the polymer matrix increases the thermodynamic instability of the cast film and thus leads to instantaneous demixing during membrane formation, which in turn causes the formation of macrovoids (Smolders et al. 1992). On the other hand, the tangling effect of the long cellulose nanofibers promoted an increase in the overall viscosity of the cast film, causing an opposite effect on the demixing process. This tangling effect in the CA solution may slow down the solvent and non-solvent flow exchange rate during membrane formation, retarding the demixing process. As a consequence, there was a hindering of macrovoid formation (Fig. 2e).

The hydrophilicity of the top membrane surfaces was evaluated by measuring the water contact angle (Table 2). The membranes prepared in this work presented a typical hydrophilic surface contact angle value (54 ± 3 °C); nevertheless, no significant differences in the values with the addition of CNF could be observed.

Non-solvent phase inversion process is one of the most used methods for membrane preparation and the use of additives promotes changes in the material porosity generated during the phase inversion process, as previously observed in the membrane morphology. The pure CA and CA/CNF composite membrane porosity values are shown in Fig. 3. Composite membranes showed a porosity increase compared to the pure CA membrane; however, the porosity was not significantly influenced by the amount of CNF added. Composite membranes containing inorganic nanoparticles (TiO_2) (Asgarkhani et al. 2013) or amphiphilic cellulose (Gao et al. 2014) also presented an increase in porosity. As explained by Gao et al. (2014), the strong pore-forming effect of an amphiphilic modifier (cellulose) is due to the increase of water penetration into the casting solution. At the same time, as the membrane surface layer is formed, the solvent flow into the water bath is hindered, which causes the formation of membrane structures with large pores.

Changes in membrane morphology and porosity caused by additive incorporation promoted changes in water flux throughout the membrane, as can also be seen in Fig. 3. It is clear that the pure water flux increased significantly when the CNF was added to the membranes, changing from $40 \text{ L m}^{-2} \text{ h}^{-1}$ for pure CA to $880 \text{ L m}^{-2} \text{ h}^{-1}$ for CA/CNF5.0. Water flux value

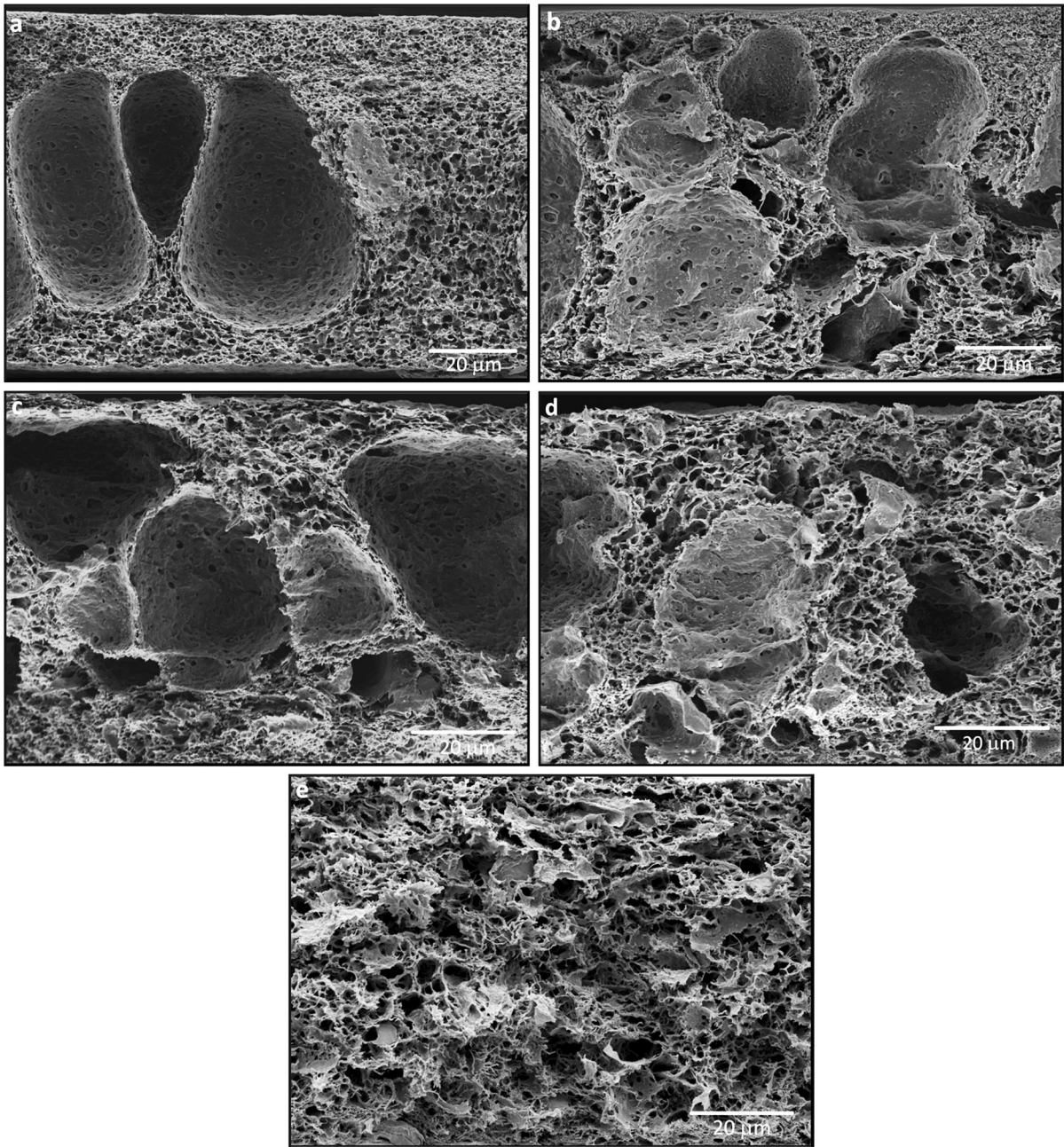


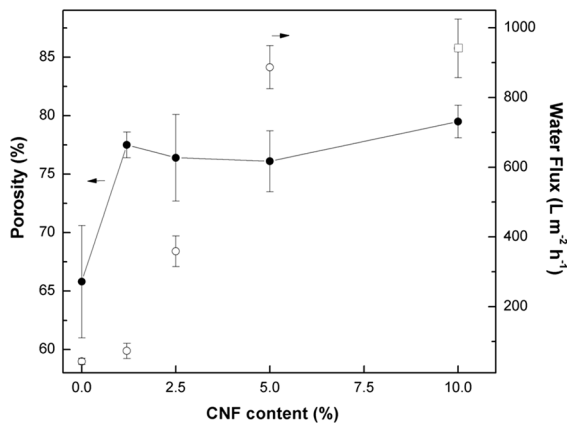
Fig. 2 SEM images of membrane cross-sections: **a** CA, **b** CA/CNF1.2, **c** CA/CNF2.5, **d** CA/CNF5.0 and **e** CA/CNF10.0

for the CA/CNF10.0 membrane ($940 \text{ L m}^{-2} \text{ h}^{-1}$ obtained at 3 bar pressure) can be explained by the formation of a sponge like structure with greater pore sizes when compared to the other membranes prepared.

In general, studies show that the presence of additives changes the membrane morphology and, consequently, water flux values (Arthanareeswaran et al. 2004; Saljoughi and Mohammadi 2009). In the case of CA, common additives are hydrophilic polymers, such as polyvinylpyrrolidone and polyethylene

Table 2 Molecular weight cut-offs, PEG retentions, PEG solution fluxes (measured at 10 bar pressure) and contact angle values of the membranes

Membrane	MWCO (kg mol ⁻¹)	PEG retention (%)	PEG solution flux (L m ⁻² h ⁻¹)	Water contact angle (°)
CA	35	86 ± 1	19 ± 7	54 ± 3
CA/CNF1.2	200	81 ± 2	16 ± 6	54 ± 2
CA/CNF2.5	200	85 ± 7	182 ± 28	59 ± 3
CA/CNF5.0	200	83 ± 3	127 ± 40	57 ± 5
CA/CNF10.0	>200	–	–	60 ± 3

**Fig. 3** CA and CA/CNF composite membrane porosity and water flux measured at 10 bar pressure. CA/CNF10.0 membrane water flux was measured at 3 bar pressure (open square symbol)

glycol. These additives are usually chosen due to presenting high affinity with the casting solvents, low affinity with the membrane forming polymer and high solubility in the non-solvent (water) so as to promote changes in the rate of polymer solution demixing during membrane formation and, consequently, in the membrane porous structure (Geburu and Das 2017). Therefore, the final membrane morphology is dependent, among other preparation variables, on the hydrophilic character of the additive as well as on the overall solution viscosity. In the present work, the fiber hydrophilicity and specially the entanglement of the long fibers in the polymer solution, caused significant visible changes in membrane morphology, as observed by SEM. Changes in the final membrane morphology were also observed by the addition of TiO₂ (Abedini et al. 2011) and SiO₂ (Arthanareswaran et al. 2008) nanoparticles as well as oxidized CNF (Kong et al. 2014) in the CA membrane.

Values of MWCO for the membranes are shown in Table 2. The MWCO value obtained for the CA membrane was 35 kg mol⁻¹. Similar MWCO values for CA membranes are reported in literature (Mahendran et al. 2002; Sivakumar et al. 2006). On the other hand, composite membranes showed higher MWCO values, compared to pure CA. This result had a good correlation with the morphological changes (Fig. 2) and porosity values observed (Fig. 3).

The CA/CNF10.0 membrane showed a very low retention value for the 200 kg mol⁻¹ PEG solution (not shown); therefore, the MWCO for this membrane can be considered higher than 200 kg mol⁻¹. Interestingly, the fact that the MWCO values were the same for membranes containing 1.2, 2.5 and 5.0% CNF can be used to infer that there were no significant changes in the top layer porosity. On the other hand, the lower values of the PEG solution fluxes, when compared to pure water flux, can be due to a concentration polarization effect during filtration tests. As well known in literature and practice, during filtration experiments the solution fluxes are generally lower than the pure water flux predicted value due to concentration polarization of solute at the membrane surface. In addition, irreversible fouling, caused by complex physical and chemical interactions between feed constituents and membrane surface, can occur simultaneously (Zydney and Colton 1986; Sablani et al. 2001; van Reis and Zydney 2007; Guo et al. 2012). However, the flux values obtained in this work are still appropriate for tests under practical conditions.

In this work, CA/CNF5 membranes were used to clarify different fruit juices and whey. In a frontal module, juice microfiltration process, feed, permeate and retentate were monitored regarding total solids, soluble solids, color, pH, turbidity, antioxidant

capacity and total phenolics. Results are presented in Table 3. The CA/CNF5 composite membrane was chosen to be tested in these experiments since it presented a high MWCO and water flux (Table 2; Fig. 3). During filtration tests using CA/CNF5 membranes, strawberry and raspberry juices presented average 630 ± 390 and $810 \pm 370 \text{ kg m}^{-2} \text{ h}^{-1}$ fluxes, respectively.

Whey feed, permeate and retentate were monitored regarding total solids, soluble solids, color, pH and turbidity during membrane separation in the dead-end cell and tangential module using the CA/CNF5 membrane. In Table 4, whey permeate and retentate showed reduced total solids content in relation to the feed stream of 18% and 3%, respectively. This result indicates that some of the initial solids were deposited in the membranes. Retentate turbidity was 11% higher after the separation process, suggesting that concentration of whey cloudiness-causing components has occurred. Finally, color results showed that the whey was lighter after treatment. Qiu et al. (2015) also found out that microfiltration resulted in a lighter whey product, which was probably due to small particle removal. No statistical difference was found for pH (4.47), soluble solids and the b^* color parameter in all the whey samples for the experiments in the dead-end module. In the tangential module, statistical differences were only found for soluble solids and the L color parameter. A 4% decrease in soluble solids was found for the permeate in relation to the feed. The results of L^* parameter did not present similar values to those of the whey treated in a dead-end module. Average whey permeation flux in the tangential module was about 6 times higher ($880 \pm 350 \text{ kg m}^{-2} \text{ h}^{-1}$) than that obtained in the dead-end module apparatus ($145 \pm 39 \text{ kg m}^{-2} \text{ h}^{-1}$).

Permeated strawberry juices presented a 41% decrease in total solids and a 34% decrease in soluble solids in relation to feed stream. This indicates that solids are being retained by the membranes. These results are in agreement with turbidity, which presented a 71% decrease after treatment. Total phenolics decreased 19% between permeated and feed streams but no changes were observed in the antioxidant capacity as well as in pH (3.53) of the permeate. After the membrane process, strawberry juices presented a darker, less red and less yellow color.

A 39% decrease in total solids was found for raspberry juice samples. No changes, however, were

Table 3 Physical-chemical parameters of fruit juices after filtration using a CA/CNF5 membrane in a dead-end filtration cell

	Total solids (%)	Soluble Solids ($^{\circ}\text{Bx}$)	Turbidity (AU*)	Total phenolics (mg mL $^{-1}$)	Antioxidant capacity (10 3 mg mL $^{-1}$)	L*value	a*value	b*value
Strawberry								
Feed	2.01 ± 0.15^a	2.95 ± 0.07^a	0.14 ± 0.01^a	43.02 ± 1.48^a	1.34 ± 0.02^a	5.17 ± 2.74^a	5.32 ± 0.92^a	2.49 ± 1.12^a
Retentate	1.77 ± 0.46^{ab}	2.37 ± 0.15^{ab}	0.05 ± 0.01^b	34.81 ± 1.74^b	1.20 ± 0.25^a	2.91 ± 0.58^b	3.83 ± 0.88^b	1.53 ± 0.60^b
Permeate	1.18 ± 0.34^{bc}	1.95 ± 0.49^b	0.04 ± 0.01^c	35.05 ± 4.16^{bc}	1.09 ± 0.14^a	2.69 ± 1.37^{bc}	2.89 ± 0.83^c	0.82 ± 0.45^c
Raspberry								
Feed	2.91 ± 0.26^a	2.90 ± 0.00^a	0.72 ± 0.15^a	38.10 ± 2.07^a	1.50 ± 0.35^a	4.62 ± 0.20^a	11.98 ± 0.51^a	2.86 ± 0.25^a
Retentate	2.11 ± 0.53^b	2.57 ± 0.38^a	0.36 ± 0.19^b	32.59 ± 3.59^a	1.26 ± 0.25^a	3.72 ± 0.21^b	8.75 ± 0.53^b	1.74 ± 0.11^b
Permeate	1.77 ± 0.51^{bc}	2.55 ± 0.07^a	0.16 ± 0.06^c	36.55 ± 7.58^a	1.21 ± 0.06^a	3.11 ± 0.09^c	8.38 ± 0.07^{bc}	2.30 ± 0.10^c

Different letters indicate that means significantly differ at $p < 0.05$. *AU absorbance units

Table 4 Physical-chemical parameters of whey before and after filtration using a CA/CNF5 membrane

	Total solids (%)	Soluble solids (°Bx)	Turbidity (AU*)	L*value	a*value	b*value
Dead-end						
Feed	7.17 ± 0.09 ^a	7.40 ± 0.14 ^a	0.09 ± 0.01 ^a	11.61 ± 1.11 ^a	-1.61 ± 0.16 ^a	-1.38 ± 0.36 ^a
Retentate	6.93 ± 0.57 ^{ab}	7.48 ± 0.60 ^a	0.10 ± 0.01 ^b	13.74 ± 0.94 ^b	-1.39 ± 0.23 ^b	-0.74 ± 1.12 ^a
Permeate	5.86 ± 1.07 ^c	6.88 ± 0.85 ^a	0.07 ± 0.04 ^{ab}	13.88 ± 0.37 ^{bc}	-1.33 ± 0.12 ^{bc}	-0.61 ± 0.53 ^a
Tangential						
Feed	5.01 ± 0.05 ^a	6.35 ± 0.07 ^{ab}	0.13 ± 0.02 ^a	13.46 ± 0.46 ^{ab}	-1.27 ± 0.22 ^a	-0.40 ± 0.38 ^a
Retentate	5.25 ± 0.16 ^a	6.20 ± 0.00 ^a	0.13 ± 0.04 ^a	13.60 ± 0.17 ^a	-1.24 ± 0.21 ^a	-0.37 ± 0.31 ^a
Permeate	5.02 ± 0.10 ^a	6.10 ± 0.00 ^b	0.11 ± 0.01 ^a	13.34 ± 0.25 ^b	-1.32 ± 0.20 ^a	-0.53 ± 0.30 ^a

Different letters indicate that means significantly differ at $p < 0.05$. *AU absorbance units

observed for soluble solids, total phenolics, pH (3.33) and antioxidant capacity in this juice. Turbidity decreased after treatment by 78%. Color changes followed the same tendency of strawberry juices, resulting in a darker, shifting towards a less red and yellow juice. Microfiltration was also more effective in producing less turbid red raspberry juice when compared to flocculation-like processes, as shown by Vladislavljević et al. (2013). These results showed an advantage in using composite membranes for juice clarification compared to pure CA membrane that was not able to perform juice clarification, due to its lower permeate flux and smaller MWCO value. The turbidity values represent a clearer juice, with turbidity loss at around 70% for strawberry and raspberry.

The attractive color is one of the main sensory characteristics of fruit juices. In this work, juice color was characterized according to the L*, a*, and b* color parameters in the CIELab uniform color space. For the evaluation of color, the parameter difference in color (ΔE) was calculated. The difference in color observed for the samples was quite small with values of $\Delta E = 0.91$ for raspberry juice and $\Delta E = 1.20$ for strawberry. These results indicate that the majority of the anthocyanins, which are responsible for the color of the juice, were maintained after the separation process (Rein and Heinonen 2004; Segovia-Bravo et al. 2012; Arend et al. 2017).

Therefore, the CA/CNF5 membranes showed good performance in both the permeate flux and clarified product quality. Although total solids were not completely removed from permeates, it was possible to observe a decrease of turbidity and the maintenance of color for clarified juices and whey.

Conclusions

The addition of CNF in the CA solution, led to different composite membrane morphologies. Formation of macrovoids was observed in the pure CA membrane. The addition of 1.25 and 2.5 wt% CNF accelerated the casting solution demixing process, promoting an increase in the membrane macrovoid mean diameter. However, using 5.0 and 10.0 wt% CNF contents promoted a higher delay in the demixing phase-separation process, which caused a reduction and also suppression of macrovoid formation and gave rise to preferentially sponge-like structures. These morphological modifications with CNF incorporation affected membrane porosity and hydrophilicity, which resulted in the improvement of pure water and PEG solution fluxes through the composite membranes and consequently an increase in the membrane molecular weight cut-offs. These special membrane characteristics can be useful for applications where high flux is required. As shown by the presented results, the use of the CA/CNF5.0 composite membrane allowed fruit juice (strawberry and raspberry) and whey clarification due to the decrease of turbidity, that of solids, and the maintenance of antioxidant capacity, as well as that of overall color.

Acknowledgments The authors are grateful to the São Paulo State Research Foundation (FAPESP), the National Council for Technological and Scientific Development (CNPq), CAPES Foundation and the National Institute of Science, Technology and Innovation in Complex Functional Materials (INOMAT/INCT) for their financial support. The authors would also like to thank Suzano Papel e Celulose S.A., Limeira, Brazil for cellulose nanofiber donation.

References

- Abdul Khalil HPS, Davoudpour Y, Islam MN et al (2014) Production and modification of nanofibrillated cellulose using various mechanical processes: a review. *Carbohydr Polym* 99:649–665. doi:[10.1016/j.carbpol.2013.08.069](https://doi.org/10.1016/j.carbpol.2013.08.069)
- Abedini R, Mousavi SM, Aminzadeh R (2011) A novel cellulose acetate (CA) membrane using TiO₂ nanoparticles: preparation, characterization and permeation study. *Desalination* 277:40–45. doi:[10.1016/j.desal.2011.03.089](https://doi.org/10.1016/j.desal.2011.03.089)
- Antrade PF, de Faria AF, Quites FJ et al (2015) Inhibition of bacterial adhesion on cellulose acetate membranes containing silver nanoparticles. *Cellulose* 22:3895–3906. doi:[10.1007/s10570-015-0752-6](https://doi.org/10.1007/s10570-015-0752-6)
- Arend GD, Adorno WT, Rezzadori K et al (2017) Concentration of phenolic compounds from strawberry (*Fragaria X ananassa* Duch) juice by nanofiltration membrane. *J Food Eng* 201:36–41. doi:[10.1016/j.jfoodeng.2017.01.014](https://doi.org/10.1016/j.jfoodeng.2017.01.014)
- Arthanareswaran G, Thanikaivelan P, Srinivasn K et al (2004) Synthesis, characterization and thermal studies on cellulose acetate membranes with additive. *Eur Polym J* 40:2153–2159. doi:[10.1016/j.eurpolymj.2004.04.024](https://doi.org/10.1016/j.eurpolymj.2004.04.024)
- Arthanareswaran G, Devi TKS, Raajenthiren M (2008) Effect of silica particles on cellulose acetate blend ultrafiltration membranes: part I. *Sep Purif Technol* 64:38–47. doi:[10.1016/j.seppur.2008.08.010](https://doi.org/10.1016/j.seppur.2008.08.010)
- Asgarkhani MAH, Mousavi SM, Saljoughi E (2013) Cellulose acetate butyrate membrane containing TiO₂ nanoparticle: preparation, characterization and permeation study. *Korean J Chem Eng* 30:1819–1824. doi:[10.1007/s11814-013-0122-8](https://doi.org/10.1007/s11814-013-0122-8)
- Association of Official Analytical Chemists (2006) Official methods of analysis of the association of official analytical chemists, 18th edition, Howitz W, (ed), George W. Latimer Jr., assistant editor, Gaithersburg, MD, USA
- Aulin C, Gällstedt M, Lindström T (2010) Oxygen and oil barrier properties of microfibrillated cellulose films and coatings. *Cellulose* 17:559–574. doi:[10.1007/s10570-009-9393-y](https://doi.org/10.1007/s10570-009-9393-y)
- Belleville M, Vaillant F (2015) Membrane technology for production of nutraceuticals. Functional food ingredients and nutraceuticals. Taylor & Francis Group, LLC, Boca Raton, pp 217–234
- Benzie IFF, Strain JJ (1996) The ferric reducing ability of plasma (FRAP) as a measure of “antioxidant power”: the FRAP assay. *Anal Biochem* 239:70–76. doi:[10.1006/abio.1996.0292](https://doi.org/10.1006/abio.1996.0292)
- Campos PRF, Módenes AN, Espinoza-Quiñones FR et al (2016) Improvement on the concentrated grape juice physico-chemical characteristics by an enzymatic treatment and membrane separation processes. *An Acad Bras Cienc* 88:423–436. doi:[10.1590/0001-3765201620140136](https://doi.org/10.1590/0001-3765201620140136)
- Chen Z, Deng M, Chen Y et al (2004) Preparation and performance of cellulose acetate/polyethyleneimine blend microfiltration membranes and their applications. *J Memb Sci* 235:73–86. doi:[10.1016/j.memsci.2004.01.024](https://doi.org/10.1016/j.memsci.2004.01.024)
- Divrikli U, Kartal A, Soylak M, Elci L (2007) Preconcentration of Pb(II), Cr(III), Cu(II), Ni(II) and Cd(II) ions in environmental samples by membrane filtration prior to their flame atomic absorption spectrometric determinations. *J Hazard Mater* 145:459–464. doi:[10.1016/j.jhazmat.2006.11.040](https://doi.org/10.1016/j.jhazmat.2006.11.040)
- Fortunato G, Zimmermann T, Lübber J et al (2012) Reinforcement of polymeric submicrometer-sized fibers by microfibrillated cellulose. *Macromol Mater Eng* 297:576–584. doi:[10.1002/mame.201100408](https://doi.org/10.1002/mame.201100408)
- Fukuzumi H, Saito T, Iwata T et al (2009) Transparent and high gas barrier films of cellulose nanofibers prepared by TEMPO-mediated oxidation. *Biomacromol* 10:162–165. doi:[10.1021/bm801065u](https://doi.org/10.1021/bm801065u)
- Gao Y, Li B, Zhong L et al (2014) Effect of nano-amphiphilic cellulose as a modifier to PSf composite membranes. *Vacuum* 107:199–203. doi:[10.1016/j.vacuum.2014.01.029](https://doi.org/10.1016/j.vacuum.2014.01.029)
- Gebru KA, Das C (2017) Effects of solubility parameter differences among PEG, PVP and CA on the preparation of ultrafiltration membranes: impacts of solvents and additives on morphology, permeability and fouling performances. *Chinese J Chem Eng* 25:911–923. doi:[10.1016/j.cjche.2016.11.017](https://doi.org/10.1016/j.cjche.2016.11.017)
- Ghosh R (2008) Ultrafiltration-based protein bioseparation. In: Pabby AK, Rizvi SSH, Sastre AM (eds) Handbook of membrane separations. CRC Press, Boca Raton, pp 497–511
- Gökmen V, Artık N, Acar J et al (2001) Effects of various clarification treatments on patulin, phenolic compound and organic acid compositions of apple juice. *Eur Food Res Technol* 213:194–199. doi:[10.1007/s002170100354](https://doi.org/10.1007/s002170100354)
- Guillen GR, Pan Y, Li M, Hoek EMV (2011) Preparation and characterization of membranes formed by nonsolvent induced phase separation: a review. *Ind Eng Chem Res* 50:3798–3817. doi:[10.1021/ie101928r](https://doi.org/10.1021/ie101928r)
- Guo W, Ngo H-H, Li J (2012) A mini-review on membrane fouling. *Bioresour Technol* 122:27–34. doi:[10.1016/j.biortech.2012.04.089](https://doi.org/10.1016/j.biortech.2012.04.089)
- Han B, Zhang D, Shao Z et al (2013) Preparation and characterization of cellulose acetate/carboxymethyl cellulose acetate blend ultrafiltration membranes. *Desalination* 311:80–89. doi:[10.1016/j.desal.2012.11.002](https://doi.org/10.1016/j.desal.2012.11.002)
- He Z, Meng M, Yan L et al (2015) Fabrication of new cellulose acetate blend imprinted membrane assisted with ionic liquid ([BMIM]Cl) for selective adsorption of salicylic acid from industrial wastewater. *Sep Purif Technol* 145:63–74. doi:[10.1016/j.seppur.2015.03.005](https://doi.org/10.1016/j.seppur.2015.03.005)
- Huang M-R, Li X-G (1998) Thermal degradation of cellulose and cellulose esters. *J Appl Polym Sci* 68:293–304. doi:[10.1002/\(SICI\)1097-4628\(19980411\)68:2<293:AID-APP11>3.0.CO;2-Z](https://doi.org/10.1002/(SICI)1097-4628(19980411)68:2<293:AID-APP11>3.0.CO;2-Z)
- Iwatake A, Nogi M, Yano H (2008) Cellulose nanofiber-reinforced polylactic acid. *Compos Sci Technol* 68:2103–2106. doi:[10.1016/j.compscitech.2008.03.006](https://doi.org/10.1016/j.compscitech.2008.03.006)
- Kalia S, Boufi S, Celli A, Kango S (2014) Nanofibrillated cellulose: surface modification and potential applications. *Colloid Polym Sci* 292:5–31. doi:[10.1007/s00396-013-3112-9](https://doi.org/10.1007/s00396-013-3112-9)
- Kong L, Zhang D, Shao Z et al (2014) Superior effect of TEMPO-oxidized cellulose nanofibrils (TOCNs) on the performance of cellulose triacetate (CTA) ultrafiltration membrane. *Desalination* 332:117–125. doi:[10.1016/j.desal.2013.11.005](https://doi.org/10.1016/j.desal.2013.11.005)

- Kunst B, Sourirajan S (1974) An approach to the development of cellulose acetate ultrafiltration membranes. *J Appl Polym Sci* 18:3423–3434. doi:[10.1002/app.1974.070181121](https://doi.org/10.1002/app.1974.070181121)
- Kutowy O, Sourirajan S (1975) Cellulose acetate ultrafiltration membranes. *J Appl Polym Sci* 19:1449–1460. doi:[10.1002/app.1975.070190525](https://doi.org/10.1002/app.1975.070190525)
- Lalia BS, Kochkodan V, Hashaikheh R, Hilal N (2013) A review on membrane fabrication: structure, properties and performance relationship. *Desalination* 326:77–95. doi:[10.1016/j.desal.2013.06.016](https://doi.org/10.1016/j.desal.2013.06.016)
- Mahendran R, Malaisamy R, Mohan D (2002) Cellulose acetate and epoxy resin blend ultrafiltration membranes: preparation, characterization, and application. *J Macromol Sci Part A* 39:1025–1035. doi:[10.1081/MA-120013577](https://doi.org/10.1081/MA-120013577)
- Nogi M, Iwamoto S, Nakagaito AN, Yano H (2009) Optically transparent nanofiber paper. *Adv Mater* 21:1595–1598. doi:[10.1002/adma.200803174](https://doi.org/10.1002/adma.200803174)
- Özgür Seydibeyoğlu M, Oksman K (2008) Novel nanocomposites based on polyurethane and micro fibrillated cellulose. *Compos Sci Technol* 68:908–914. doi:[10.1016/j.compscitech.2007.08.008](https://doi.org/10.1016/j.compscitech.2007.08.008)
- Perera DHN, Nataraj SK, Thomson NM et al (2014) Room-temperature development of thin film composite reverse osmosis membranes from cellulose acetate with antibacterial properties. *J Memb Sci* 453:212–220. doi:[10.1016/j.memsci.2013.10.062](https://doi.org/10.1016/j.memsci.2013.10.062)
- Qiu Y, Smith TJ, Foegeding EA, Drake MA (2015) The effect of microfiltration on color, flavor, and functionality of 80% whey protein concentrate. *J Dairy Sci* 98:5862–5873. doi:[10.3168/jds.2014-9174](https://doi.org/10.3168/jds.2014-9174)
- Rein MJ, Heinonen M (2004) Stability and enhancement of berry juice color. *J Agric Food Chem* 52:3106–3114. doi:[10.1021/jf035507i](https://doi.org/10.1021/jf035507i)
- Reuvers AJ, Smolders CA (1987) Formation of membranes by means of immersion precipitation. *J Memb Sci* 34:67–86. doi:[10.1016/S0376-7388\(00\)80021-6](https://doi.org/10.1016/S0376-7388(00)80021-6)
- Roman M, Winter WT (2004) Effect of sulfate groups from sulfuric acid hydrolysis on the thermal degradation behavior of bacterial cellulose. *Biomacromol* 5:1671–1677. doi:[10.1021/bm034519+](https://doi.org/10.1021/bm034519+)
- Rufino MSMC, Alves RE, Sousa de Brito E, et al (2006) Metodologia científica: determinação da atividade antioxidante total em frutas pelo Método de Redução do Ferro (FRAP)
- Sabeti Dehkordi F, Pakizeh M, Namvar-Mahboub M (2015) Properties and ultrafiltration efficiency of cellulose acetate/organically modified Mt (CA/OMMt) nanocomposite membrane for humic acid removal. *Appl Clay Sci* 105–106:178–185. doi:[10.1016/j.clay.2014.11.042](https://doi.org/10.1016/j.clay.2014.11.042)
- Sablani S, Goosen M, Al-Belushi R, Wilf M (2001) Concentration polarization in ultrafiltration and reverse osmosis: a critical review. *Desalination* 141:269–289. doi:[10.1016/S0011-9164\(01\)85005-0](https://doi.org/10.1016/S0011-9164(01)85005-0)
- Saljoughi E, Mohammadi T (2009) Cellulose acetate (CA)/polyvinylpyrrolidone (PVP) blend asymmetric membranes: preparation, morphology and performance. *Desalination* 249:850–854. doi:[10.1016/j.desal.2008.12.066](https://doi.org/10.1016/j.desal.2008.12.066)
- Segovia-Bravo KA, Guignon B, Bermejo-Prada A et al (2012) Hyperbaric storage at room temperature for food preservation: a study in strawberry juice. *Innov Food Sci Emerg Technol* 15:14–22. doi:[10.1016/j.ifset.2012.02.005](https://doi.org/10.1016/j.ifset.2012.02.005)
- Silva VM, Sato ACK, Barbosa G et al (2010) The effect of homogenisation on the stability of pineapple pulp. *Int J Food Sci Technol* 45:2127–2133. doi:[10.1111/j.1365-2621.2010.02386.x](https://doi.org/10.1111/j.1365-2621.2010.02386.x)
- Singleton VL Jr, Rossi JA (1965) Colorimetry of total phenolics with phosphomolybdic-phosphotungstic acid reagents. *Am J Enol Vitic* 16:144–158
- Sivakumar M, Mohan DR, Rangarajan R (2006) Studies on cellulose acetate-polysulfone ultrafiltration membranes. *J Memb Sci* 268:208–219. doi:[10.1016/j.memsci.2005.06.017](https://doi.org/10.1016/j.memsci.2005.06.017)
- Smolders CA, Reuvers AJ, Boom RM, Wienk IM (1992) Microstructures in phase-inversion membranes. Part 1. Formation of macrovoids. *J Memb Sci* 73:259–275. doi:[10.1016/0376-7388\(92\)80134-6](https://doi.org/10.1016/0376-7388(92)80134-6)
- Soylak M, Divrikli U, Elci L, Dogan M (2002) Preconcentration of Cr(III), Co(II), Cu(II), Fe(III) and Pb(II) as calmagite chelates on cellulose nitrate membrane filter prior to their flame atomic absorption spectrometric determinations. *Talanta* 56:565–570. doi:[10.1016/S0039-9140\(01\)00575-6](https://doi.org/10.1016/S0039-9140(01)00575-6)
- Soylak M, Unsal YE, Kizil N, Aydin A (2010) Utilization of membrane filtration for preconcentration and determination of Cu(II) and Pb(II) in food, water and geological samples by atomic absorption spectrometry. *Food Chem Toxicol* 48:517–521. doi:[10.1016/j.fct.2009.11.005](https://doi.org/10.1016/j.fct.2009.11.005)
- Spence KL, Venditti RA, Rojas OJ et al (2010) The effect of chemical composition on microfibrillar cellulose films from wood pulps: water interactions and physical properties for packaging applications. *Cellulose* 17:835–848. doi:[10.1007/s10570-010-9424-8](https://doi.org/10.1007/s10570-010-9424-8)
- Takagi H, Asano A (2008) Effects of processing conditions on flexural properties of cellulose nanofiber reinforced “green” composites. *Compos Part A Appl Sci Manuf* 39:685–689. doi:[10.1016/j.compositesa.2007.08.019](https://doi.org/10.1016/j.compositesa.2007.08.019)
- Tian Y, Wu M, Liu R et al (2011) Electrospun membrane of cellulose acetate for heavy metal ion adsorption in water treatment. *Carbohydr Polym* 83:743–748. doi:[10.1016/j.carbpol.2010.08.054](https://doi.org/10.1016/j.carbpol.2010.08.054)
- van Reis R, Zydney A (2007) Bioprocess membrane technology. *J Memb Sci* 297:16–50. doi:[10.1016/j.memsci.2007.02.045](https://doi.org/10.1016/j.memsci.2007.02.045)
- Vladislavljević GT, Vukosavljević P, Veljović MS (2013) Clarification of red raspberry juice using microfiltration with gas backwashing: a viable strategy to maximize permeate flux and minimize a loss of anthocyanins. *Food Bioprod Process* 91:473–480. doi:[10.1016/j.fbp.2013.05.004](https://doi.org/10.1016/j.fbp.2013.05.004)
- Waterhouse AL (2003) Determination of total phenolics. In: Wrolstad RE (ed) *Current protocols in food analytical chemistry*. Wiley, Hoboken, pp 11.1.1–11.1.8
- Yang H, Yan R, Chen H et al (2007) Characteristics of hemi-cellulose, cellulose and lignin pyrolysis. *Fuel* 86:1781–1788. doi:[10.1016/j.fuel.2006.12.013](https://doi.org/10.1016/j.fuel.2006.12.013)
- Zydney AL, Colton CK (1986) A Concentration polarization model for the filtrate flux in cross-flow microfiltration of particulate suspensions. *Chem Eng Commun* 47:1–21. doi:[10.1080/00986448608911751](https://doi.org/10.1080/00986448608911751)